Theoretical Study on Highly Active Bifunctional Metalloporphyrin Catalysts for the Coupling Reaction of Epoxides with Carbon Dioxide

Jun-ya Hasegawa,*[a] Ray Miyazaki,[a] Chihiro Maeda,*[b] and Tadashi Ema*[b]

((Insert Picture for Frontispiece here [18.0×18.0 cm]))

Abstract: Highly active bifunctional metalloporphyrin catalysts were developed for the coupling reaction of epoxides with CO_2 to produce cyclic carbonates. The bifunctional catalysts have both quaternary ammonium halide and the metal center. To elucidate the roles of these catalytic groups, DFT calculations were performed. Control reactions using tetrabutylammonium halide as a catalyst were also investigated for comparison. In the present article, the results of our computational studies are overviewed. The computational results are consistent with the experimental data and are useful for elucidating the structure–activity relationship. The key features responsible for the high catalytic activity of the bifunctional catalysts are as follows: (1) the cooperative action of the halide anion (nucleophile) and the metal center (Lewis acid), (2) the near-attack conformation leading to the efficient opening of the epoxide ring in the rate-determining step, and (3) the conformational change of the quaternary ammonium cation to stabilize various anionic species generated during catalysis in addition to the robustness (thermostability) of the catalysts.

1. Introduction

Carbon dioxide (CO_2) is an inexpensive and abundant C1 source. It is desirable to develop efficient and useful methods for the conversion of CO_2 into value-added chemicals.[1] One of the most useful reactions is the catalytic coupling reaction of CO_2 with epoxides to produce cyclic carbonates because the products can be used as electrolytes in lithium-ion secondary batteries and as raw materials for polycarbonates and because the reaction exhibits high atom efficiency (Figure 1a). Various catalysts, including metalloporphyrins,[2][3] have been developed. The rigid porphyrin framework enables the introduction of various metal ions and functional groups. We have reported highly active bifunctional metalloporphyrin catalysts with the quaternary ammonium halide groups (Figure 1c).[3] The bifunctional catalysts have two catalytic groups: one is quaternary ammonium halide (nucleophile) at the *meta* positions of the *meso*-phenyl groups, and the other is the central metal ion (Lewis acid). The epoxide is activated by metal-coordination to facilitate nucleophilic attack as represented by Figure 1b. The bifunctional metalloporphyrins showed very high turnover frequencies (TOF) and turnover numbers (TON) (Figure 1c).

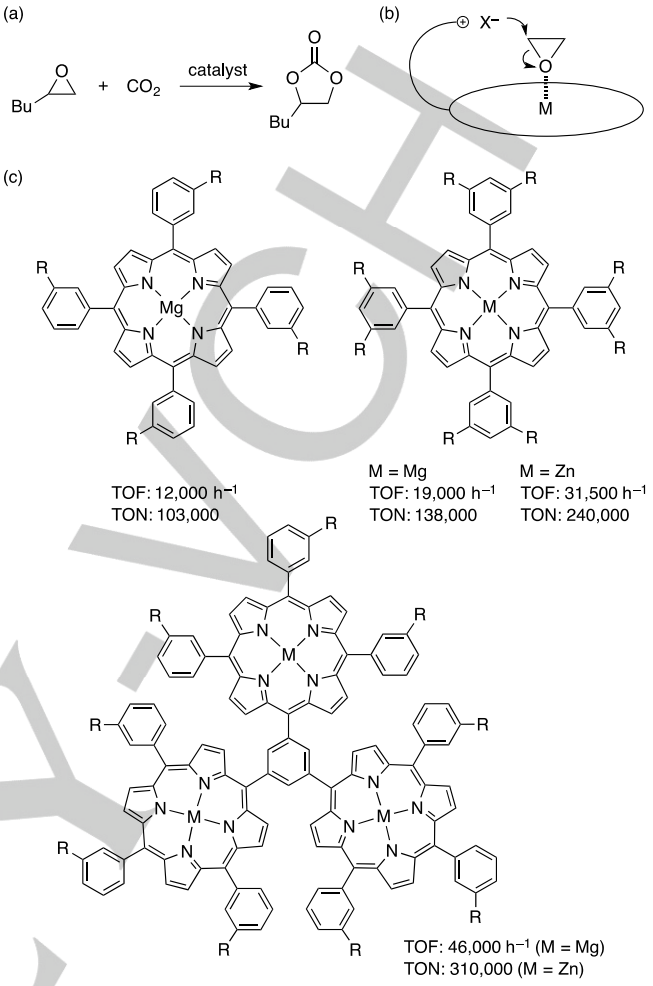

Figure 1. a) Synthesis of cyclic carbonate from epoxide and CO_2. b) Schematic representation for the activation of epoxide by bifunctional metalloporphyrins. c) Structures of bifunctional metalloporphyrin catalysts. R = $O(CH_2)_6N^+Bu_3Br^-$.

Recently, density functional theory (DFT) computational studies were published for the coupling reaction of epoxides with CO_2 to produce cyclic carbonates.[4] For example, Sun and Zhang studied alkylmethylimidazolium chloride catalysts and pointed out that the initial ring-opening reaction is the rate-determining step.[4a] They also pointed out that hydrogen bonding between the epoxide and the imidazolium cation can significantly reduce the activation barrier.[4a] However, most of the theoretical studies were focused on two-component catalytic systems. Therefore, the comparison of the optimized structures between the bifunctional porphyrin catalysts and the two-component catalysts provided significant and useful insight into the origin of the structure–activity relationship.[3b, 3d, 5]

Here we summarize our theoretical studies based on the DFT calculations on the coupling reaction of epoxides with CO_2 using the highly active bifunctional metalloporphyrin catalysts. We also describe the mechanism for the reaction catalyzed by tetrabutylammonium halide (TBAX), such as TBA chloride (TBAC), TBA bromide (TBAB), and TBA iodide (TBAI). The use

[a] Prof. J. Hasegawa, R. Miyazaki
Institute for Catalysis
Hokkaido University
Kita 21 Nishi 10, Kita-ku, Sapporo, Hokkaido 001-0021, Japan
E-mail: hasegawa@cat.hokudai.ac.jp
[b] Dr. C. Maeda, Prof. T. Ema
Division of Applied Chemistry, Graduate School of Natural Science and Technology, Okayama University, Tsushima, Okayama 700-8530, Japan
E-mail: cmaeda@okayama-u.ac.jp
ema@cc.okayama-u.ac.jp

Supporting information for this article is given via a link at the end of the document.

of these simple catalysts enabled us to deeply understand the catalytic reaction although TBAX is much less efficient than the bifunctional metalloporphyrin catalysts. The origins of the high catalytic activity of the bifunctional catalysts are (1) the cooperative action of the halide ion (nucleophile) and the metal center (Lewis acid), (2) the near-attack conformation leading to the efficient opening of the epoxide ring in the rate-determining step, and (3) the conformational change of the flexible quaternary ammonium cation to stabilize various anionic species generated during catalysis in addition to the robustness (thermostability) of the catalysts.

Jun-ya Hasegawa

Ph.D. degree at Department of Synthetic Chemistry and Biological Chemistry, Graduate School of Engineering, Kyoto University in 1998. After post-doc career at Lund University, Sweden, he became assistant professor, and then lecturer at Department of Synthetic Chemistry and Biological Chemistry. In 2011, He was promoted to associate professor at Fukui Institute for Fundamental Chemistry, Kyoto University. Since 2012, he is a professor at Catalysis Research Centre (CRC), Hokkaido University. CRC has been renewed as Institute for Catalysis in 2015. His current research interest is theoretical and computational study on catalysis.

Ray Miyazaki

He belongs to master course in Graduate School of Chemical Sciences and Engineering, Hokkaido University. His current research interest is theoretical and computational study on catalytic reactions.

Chihiro Maeda

He received his doctor's degree from Kyoto University in 2010 under the supervision of Prof. Atsuhiro Osuka. In 2010, he started his academic career at Keio University as an Assistant Professor. In 2013, he moved to Okayama University and joined Prof. Tadashi Ema group. His main research topic is synthesis and application of novel porphyrin derivatives.

Tadashi Ema

He received his bachelor's degree from Kyoto University in 1989, and he obtained his master's degree in 1991 and doctor's degree in 1994 at Kyoto University under the supervision of Professor Hisanobu Ogoshi. He was appointed as an Assistant Professor at Okayama University in 1994 and was promoted to an Associate Professor in 2002 and a Full Professor in 2012. His research interest is the design and synthesis of unique molecular catalysts.

2. Computational details

DFT calculations were performed at the B3LYP[6]/6-31G* level. The solvation effect was included with the self-consistent reaction field (SCRF) model (polarized continuum model[7] with the solvent parameters for Et_2O). In the structural optimization, frequency calculations were performed for all the stationary points. On-the-fly *ab initio* molecular dynamics calculations (AIMD) [8] were carried out on the B3LYP/3-21G and semi-empirical PM3[9] potential energy surfaces. Solvent effect at the SCRF level was considered for the B3LYP surface, but not for the PM3 one because the SCRF calculation was unavailable for the PM3 method. Temperature was set to 500 K. Atomic population was calculated with natural population analysis.[10] All the calculations were performed with the Gaussian 09 package.[11]

3. Tetrabutylammonium Halides

3.1. Potential Energy Profile

The common features of the catalytic mechanism of these quaternary ammonium halides were reported in previous studies.[4b-d] In our study,[3b] DFT calculations on the TBAX-catalyzed reactions were performed along the catalytic cycle shown in Figure 2 using propylene oxide (PO) as a model substrate. Figure 3 shows the potential energy profile for the transformation of PO to propylene carbonate (PC) using TBAC, TBAB, or TBAI as a catalyst. In the reactant state (**R**), the halide anion forms an ion pair with the TBA cation. In the ring-opening transition state (**TS1**), however, PO is located between the TBA cation and the halide anion. Although this geometry is energetically unfavorable owing to the separation of the ion pair, the TBA cation is used to stabilize the negative charge of the O atom in **TS1**. The resulting intermediate **IM1** then undergoes CO_2 insertion at the O atom. The subsequent ring-closing reaction takes place via transition state **TS2** to give the product (**P**).

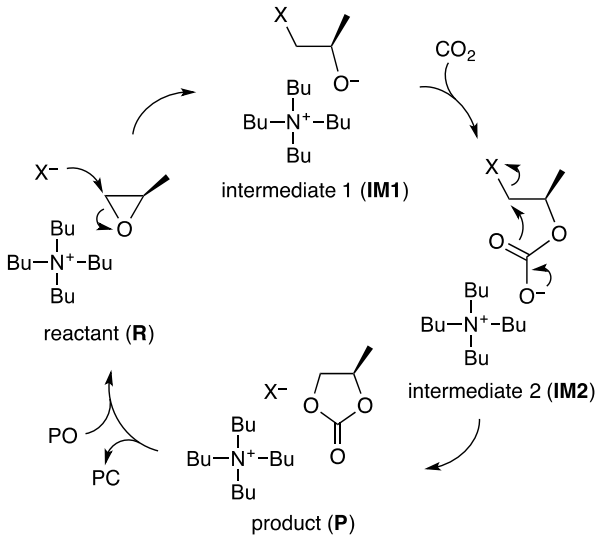

Figure 2. A catalytic cycle for the TBAX-catalyzed reaction simulated by DFT calculations.

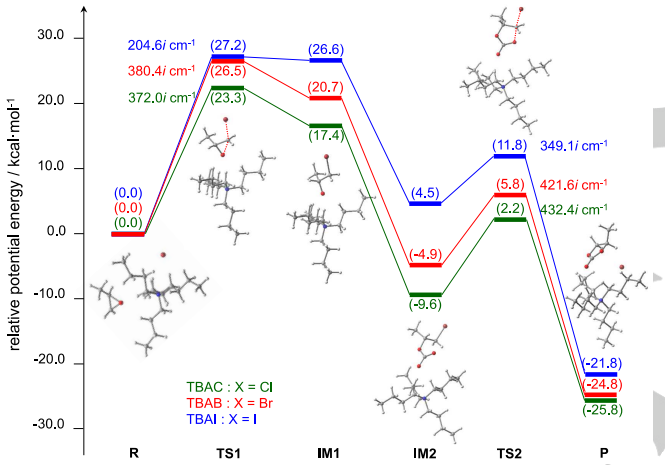

Figure 3. Potential energy profile for the conversion of propylene oxide (PO) to propylene carbonate (PC) using TBAC, TBAB, or TBAI as a catalyst. Each optimized structure in the TBAB-catalyzed reaction is also shown.

The initial ring-opening reaction is the rate-determining step because it has the highest energy and the largest energy barrier. The activation energy increases in the order TBAC (23.3 kcal/mol) < TBAB (26.5 kcal/mol) < TBAI (27.2 kcal/mol). The relative potential energy of **IM1** also increases in the order TBAC (17.4 kcal/mol) < TBAB (20.7 kcal/mol) < TBAI (26.6 kcal/mol), and **IM2** also shows the same trend. This tendency can be explained in terms of the stability of the leaving group.[3b] The I^- ion is the best leaving group, which is followed by Br^- and then Cl^-. This order is also related to the C–X bond energy. According to the literature,[12] the bond energies for C–Cl, C–Br, and C–I are 95, 67, and 50 kcal/mol, respectively.

3.2. Electrostatic Stabilization Effect by the TBA Cation

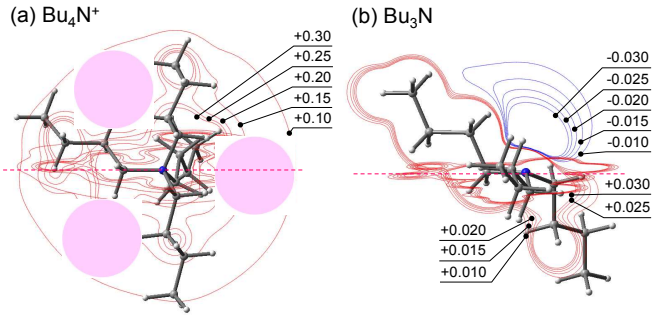

Figure 4. Electrostatic potential of (a) the TBA cation and (b) tributylamine. The isosurface in atomic unit (au) sliced at an orthogonal planes. For instance, a –1 charge on the +0.10 au surface is stabilized by 63 kcal/mol due to the electrostatic potential. Three of the four anion-binding sites in the TBA cation are shown in the pink circles.

The TBA cation has a net +1 charge that creates the positive electrostatic potential (ESP) around the catalyst. Figure 4 shows the ESP isosurfaces of the TBA cation. The spatial distribution of the positive area is nearly spherical, and the anion-binding sites are created. The natural population analysis indicated that the positive charge is located on the H atoms, but not on the N atom.[5] As a result, the positively charged H atoms of the TBA moiety can interact with various anions. We also noticed that the positive ESP decreases rapidly at the outer sphere. This property has a great effect on the stability of the anionic transition-state and intermediate species. We also calculated the ESP of a neutral variant, tributylamine, for comparison. Figure 4 clearly indicates that the magnitude of the ESP of tributylamine is much smaller than that of the TBA cation.

3.3. Orientation of Epoxide Molecule

Figure 5 shows the changes of the potential energy and the atomic charges of the Cl and O atoms upon nucleophilic attack on PO by TBAC, demonstrating the importance of the orientation of the PO molecule. Figure 5a simulates the ring opening by the Cl^- ion bound at the same position as that in the **R** state (see Figure 3). In this case, the O atom of PO is directed away from the TBA cation. The negative charge of Cl^- is shifted to the O atom as the C–Cl distance is shortened to 2.5 Å. The potential energy further increases up to a C–Cl distance of 1.9 Å, which is the ordinary C–Cl bond length; however, no stabilization arising from the C–Cl bond formation can be seen (Figure 5a). This is because the O atom (negative charge) is far from the TBA cation. In contrast, when the epoxide is inserted between the TBA cation and the Cl^- ion before opening the epoxide ring, the O atom of PO can be directed toward the TBA cation. In this case, there is an energy gain due to the electrostatic stabilization. Upon formation of the C–Cl bond, the potential energy decreases as shown in Figure 5b.

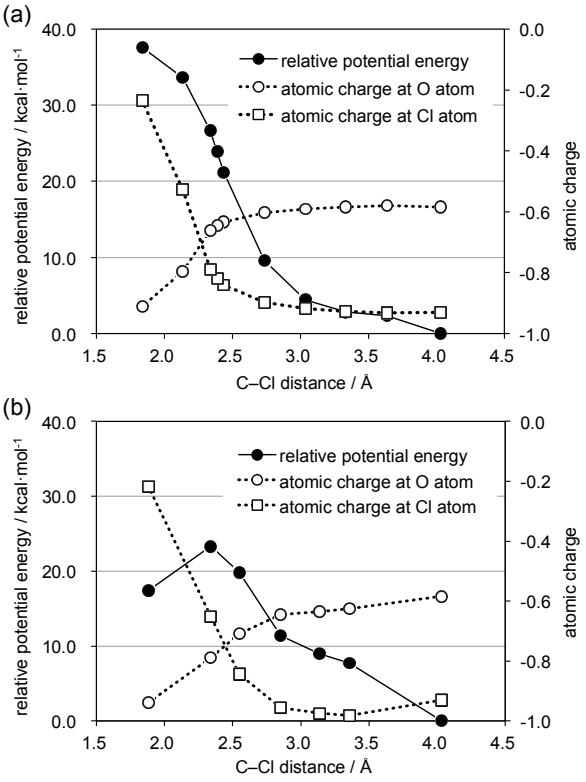

Figure 5. Potential energy curves for the PO ring opening reaction with TBAC. The O atom of PO is directed (a) away from and (b) toward the TBA cation. Natural atomic charges at the O and Cl atoms are also shown for each structure.

We next performed *ab initio* molecular dynamics (AIMD) calculations to see how far the halide anion can move away from the TBA cation. Figure S1 in Supporting Information (SI) shows that the Cl–N distance falls into 3.7–4.2 Å. We also performed AIMD calculations on the TBAB-catalyzed reaction of PO. Because the Br^- ion stays close to the TBA cation, PO has to move to another binding site by equilibrium (Figure S2). This result implies that the system has to wait for a reactive conformation that is 8 kcal/mol higher than the **R** state. Based on a simple estimation from the Boltzman distribution, only 1 out of 30,000 epoxide molecules falls into this energy level. The system needs another 15 kcal/mol to reach **TS1**. This is why the TBAX-catalyzed reactions are unfavorable.

4. Bifunctional Metalloporphyrin Catalysts

4.1. Potential Energy Profile

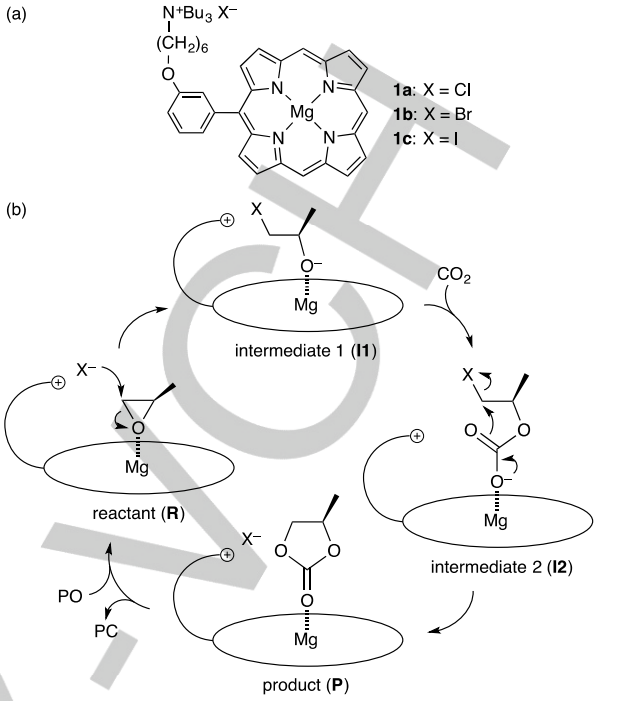

Figure 6. a) Model catalysts **1a–c** for DFT calculations. b) A catalytic cycle simulated by DFT calculations.

DFT calculations were performed along the catalytic cycle shown in Figure 6. Monosubstituted Mg(II) porphyrins **1a**, **1b**, and **1c** with different halide anions were used as model catalysts, and PO was used as a model substrate. The potential energy profile is shown in Figure 7, and the transition state and intermediate structures for the **1b**-catalyzed reaction are given in Figure 8.[3b] The catalytic reaction starts from the **R** state (Figures 6 and 7) in which the alkyl chain adopts a moderately stretched conformation (Figure 8a). The ring-opening reaction takes place, and intermediate **I1** is formed via transition state **I1_TS**. Interestingly, the calculated activation energies (E_a) increase in the order Br^- (13.5 kcal/mol) < Cl^- (16.1 kcal/mol) < I^- (20.2 kcal/mol); the reaction catalyzed by **1b** with Br^- has the smallest activation energy. This trend, which is different from that observed for TBAX (Figure 3), is in good agreement with the experimentally observed yield and TON.[3a, 3b] It is likely that the quaternary ammonium cation can stabilize the Br^- ion in the most complementary and efficient manner in transition state **I1_TS**.[3b]

As shown in Figures 8a and c, the negative charge of the Br^- ion in the **R** state is shifted to the O atom in the **I1** state. Because the charged species are separated, the quaternary ammonium cation undergoes a conformational change to a bent form, and the distance between the N and O atoms becomes closer. Starting with the lowest-energy structure of the stretched form, the AIMD trajectory shows a smooth conformational change to the bent form (Figure S2). Intermediate **I1** undergoes CO_2 attack at the negatively charged O atom. This C–O bond formation is accompanied by little or no activation barrier to

reach the second intermediate **I2**. The final step is the ring-closing reaction to give the product. The activation energies for **P_TS** are 18.0 kcal/mol (Cl), 17.1 kcal/mol (Br), and 12.3 kcal/mol (I). This order corresponds to the order of the C–X bond energy and also to the nature of the leaving group.

We also calculated the energies for the binding of PO and PC to the metal center. The calculated binding energy of the product, PC, is 10.1 kcal/mol, while that of the reactant, PO, is 11.2 kcal/mol. This result strongly suggests that the replacement of the product by the reactant easily takes place.

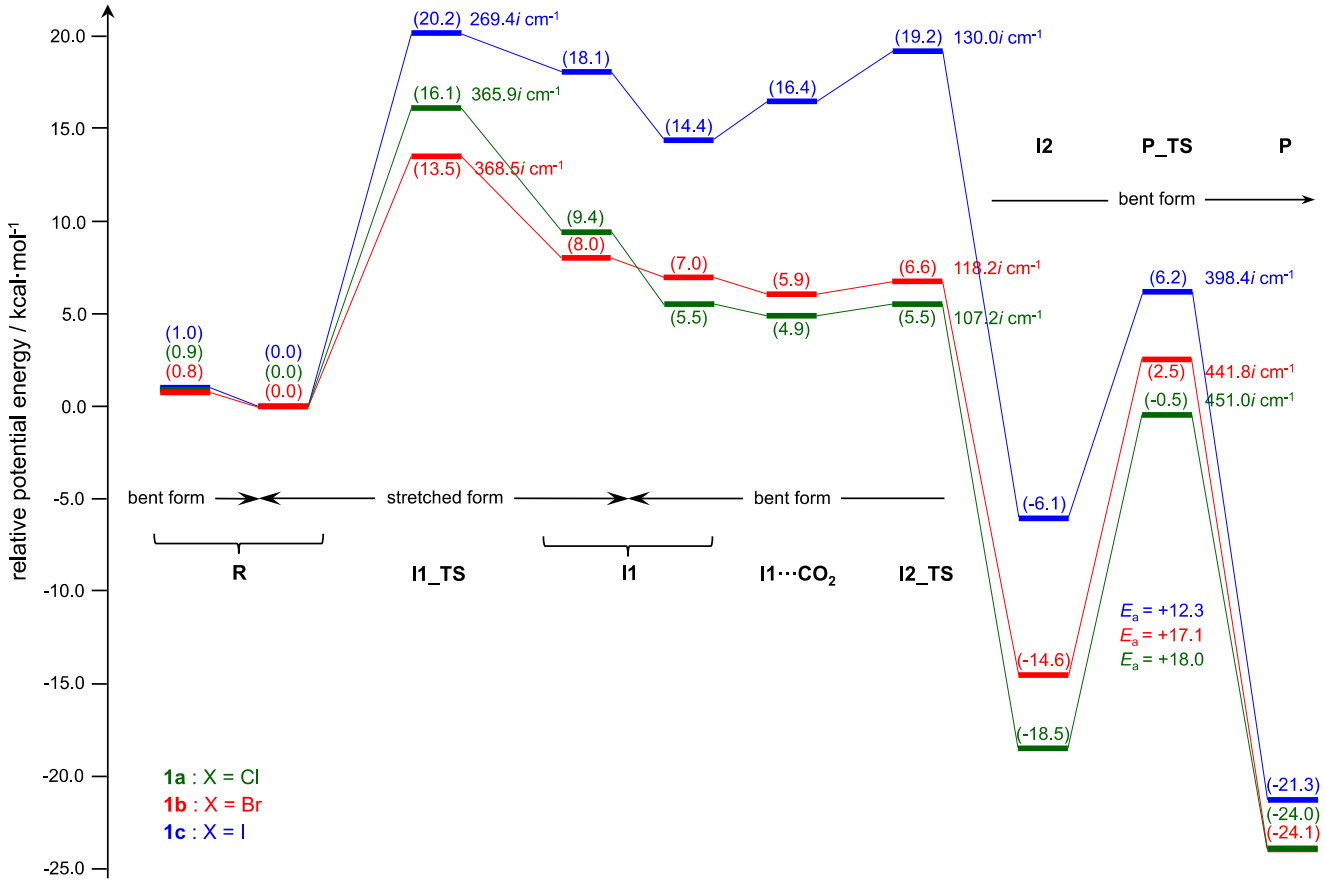

Figure 7. Potential energy profiles for the **1a**, **1b**, and **1c**-catalyzed reactions of propylene oxide (PO) with CO_2. The relative energies based on reactant **R** (stretched form) are given in kcal/mol. The energy of CO_2 is included in the former steps where CO_2 does not appear explicitly. The stretched and bent forms designated here can be seen in Figure 8. Reprinted (adapted) with permission from (T. Ema, Y. Miyazaki, J. Shimonishi, C. Maeda, and J. Hasegawa, *J. Am. Chem. Soc.* **2014**, *136*, 15270.). Copyright (2014) American Chemical Society.

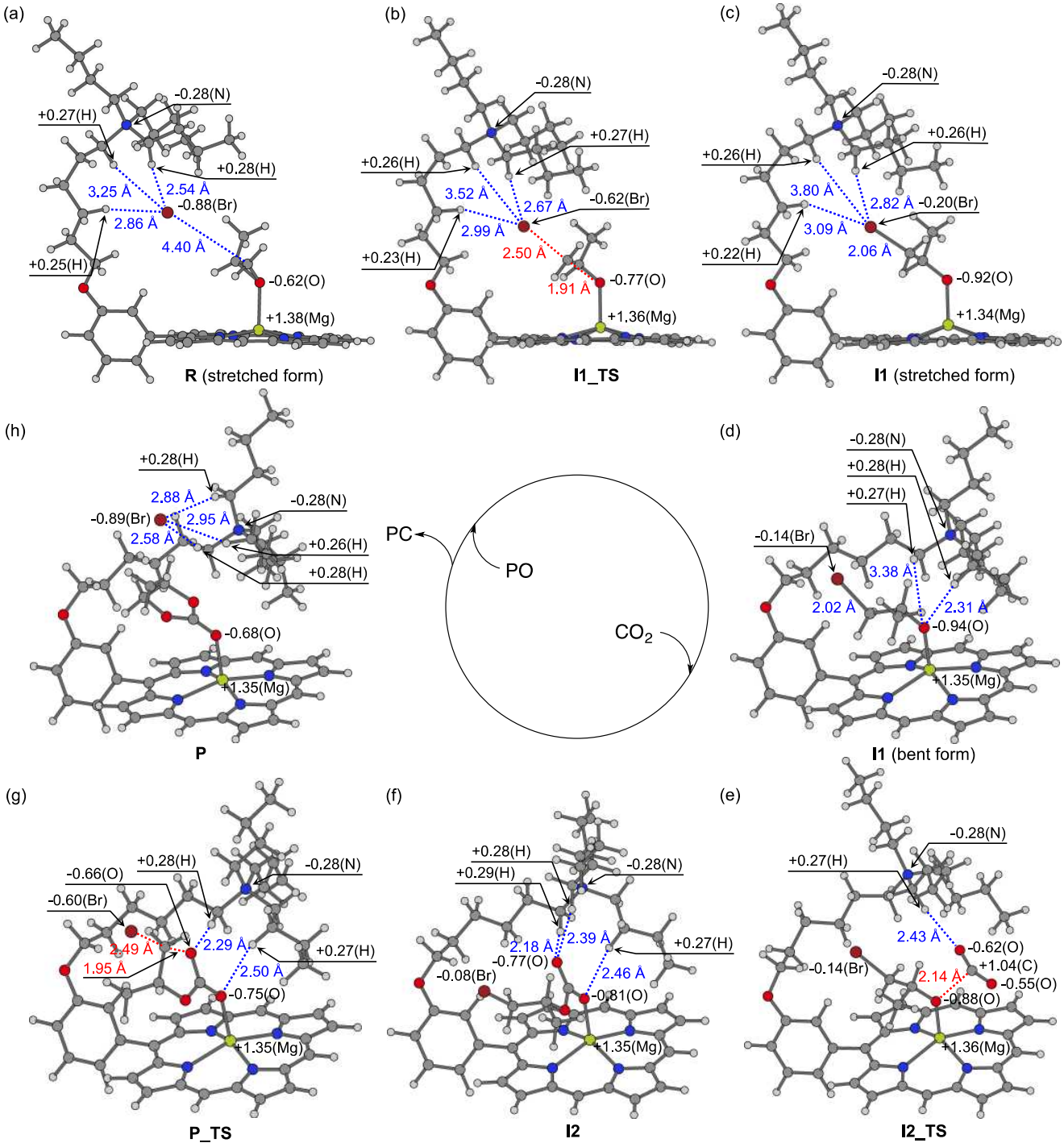

Figure 8. Optimized structures of (a) reactant **R** (stretched form), (b) transition state **I1_TS**, (c) **I1** (stretched form), (d) **I1** (bent form), (e) transition state **I2_TS**, (f) **I2**, (g) transition state **P_TS**, and (h) product **P** in the **1b**-catalyzed reaction of propylene oxide (PO) with CO_2. Reprinted (adapted) with permission from (T. Ema, Y. Miyazaki, J. Shimonishi, C. Maeda, and J. Hasegawa, *J. Am. Chem. Soc.* **2014**, *136*, 15270.). Copyright (2014) American Chemical Society.

4.2. Near-attack Conformation

The advantage of the bifunctional metalloporphyrin is structural resemblance between **R** and **I1_TS** (Figures 8a and b). Because a slight shift of the halide anion to PO in **R** can reach transition state **I1_TS**, we call the **R** state "near-attack conformation". The quaternary ammonium cation takes the "concave" conformation in **R** and **I1_TS**. We consider that this conformation increases probability to pass the activation barrier.

In contrast, in the case of TBAX, PO and X^- in **R** are located in different anion-binding sites of the TBA cation. As a result, PO is distant from the X^- ion. Even if the X^- ion and PO are close to each other, PO needs to intervene between the TBA cation and the X^- ion with an energy cost of 8 kcal/mol.

In a recent report, the role of the near-attack conformation was also proposed for the same reaction in a silica-supported niobium complex[4l]. Because the Nb complexes on the surface are in close proximity to each other, the neighboring Nb complexes bind both the epoxide and the halide anion in an ideal conformation for the ring-opening reaction.[4l]

4.3. Stability of the Ring-opened Intermediate

The Mg(II) ion of the porphyrin acts as a Lewis acid to stabilize both transition state **I1_TS** and intermediate **I1**. For example, as shown in Table 1, the potential energies for **I1_TS** and **I1** in the **1b**-catalyzed reaction are 13.5 and 8.0 kcal/mol, respectively. These values are much smaller than the corresponding values in the TBAB-catalyzed reaction (26.5 and 20.7 kcal/mol). Furthermore, intermediate **I1** undergoes the conformational change of the quaternary ammonium cation from the stretched to bent forms. Table 1 indicates that the energetic benefit caused by this conformational change is 1.0–4.0 kcal/mol, depending on the halide anion. Because the ring-opened intermediates, **IM1** for TBAX and **I1** for **1a**–**c**, undergo CO_2 attack, their lifetimes would be important for catalytic activity. As seen in Figure 5, the potential energy of the ring-opened intermediate is sensitive to the stabilization of the negatively charged O atom. Therefore, this is another advantage of the bifunctional metalloporphyrins over TBAX because in the former case, various anionic species generated during catalysis can be stabilized by both the metal center and the flexible quaternary ammonium cation (Figure 8).

Table 1. Potential energies of the transition state and intermediate in the ring-opening step relative to reactant **R**. Units are in kcal/mol.

X	TBAX		**1**		
	TS1	**IM1**	**I1_TS**	**I1** (stretched)	**I1** (bent)
Cl	23.3	17.4	16.1	9.4	5.5
Br	26.5	20.7	13.5	8.0	7.0
I	27.2	26.6	20.2	18.1	14.4

4.4. Metal Ion in the Porphyrin Ring

DFT calculations on bifunctional Zn(II) complexes were also performed, and the results were compared with that of the corresponding Mg(II) complexes.[3d] In the case of the Zn(II) complex, the calculated E_a value for the ring-opening step (14.3 kcal/mol) was slightly greater than that of the Mg(II) complex (13.5 kcal/mol). This result is in good agreement with the experimental result; the yield and TON for the Zn(II) catalysts are slightly lower than those of the Mg(II) counterparts. This difference might arise from the charge on the metal ion in **I1_TS** and **I1**. According to the NPA analysis, however, the atomic charge of Zn(II) is about +1.3 during catalysis, and this amount is only slightly less than that of the Mg(II) catalyst. Moreover, there is no significant difference in the optimized structures between the Zn(II) and Mg(II) complexes. The electronegativity or oxophilicity of the two metal ions may be important for the difference in catalytic activity. The thermostability of the Zn(II) catalyst is obviously higher than that of the Mg(II) catalyst. The TON of a Zn(II) catalyst reached 240,000 at 96% conversion after the five-day reaction.[3d]

4.5. Effect of *ortho*-, *meta*-, and *para*-Substitutions on Catalytic Activity

Considering the important role of the quaternary ammonium cation, the positional isomers of the bifunctional metalloporphyrins were synthesized and compared.[3d] As a result, *meta*-substituted catalysts showed the highest TONs in the experiments, followed by the corresponding *para* isomer and then the *ortho* isomer. To account for this experimental result, we performed the DFT calculations and compared the potential energy profiles.[3d]

The *meta* isomer has the smallest activation energy, which agrees with the experimental observation. The E_a values for the ring-opening reaction in the *ortho*-, *meta*-, and *para*-substituted catalysts are 16.4, 14.3, and 17.0 kcal/mol, respectively. In the optimized structure of the *para* isomer in the **R** state, the quaternary ammonium bromide group is stretched and directed away from the metal-coordination site. As a result, the alkyl chain linker undergoes a substantial conformational change to a reactive conformation that is 2.9 kcal/mol higher than **R**. As for the *ortho* isomer, the calculated activation energy seems to be

underestimated probably due to the insufficiency of the simplified model. In the optimized structures, the quaternary ammonium cation in the *ortho* isomer significantly invades the space of other quaternary ammonium cations on the opposite side of the porphyrin ring.

5. Summary

Highly active and robust metalloporphyrin catalysts were developed for the coupling reaction of epoxides with CO_2.[3] The bifunctional metalloporphyrins have the quaternary ammonium halide groups via the hexamethylene linker carefully optimized for the best catalytic activity. To elucidate the roles of the catalytic groups, we performed DFT calculations and obtained the potential energy profiles together with the optimized structures of the reactant, transition state, intermediate, and the product. In addition, we studied the reactions catalyzed by TBAX for comparison. Computational studies were useful for clarifying the structure–activity relationship. The origins of the high catalytic activity of the bifunctional metalloporphyrin catalysts can be summarized as follows: (1) the cooperative action of the halide ion (nucleophile) and the metal center (Lewis acid), (2) the near-attack conformation leading to the efficient opening of the epoxide ring in the rate-determining step, and (3) the conformational change of the flexible quaternary ammonium cation to stabilize various anionic species generated during catalysis in addition to the robustness (thermostability) of the catalysts.

Acknowledgements

This work was supported by the ENEOS Hydrogen Trust Fund, Okayama Foundation for Science and Technology, and Ministry of Education, Culture, Sports, Science and Technology (MEXT) in Japan. The work at Hokkaido University was supported by JSPS KAKENHI Grant Number 15H05805 and the FLAGSHIP2020 (priority study 5) program from MEXT. Computations were partly carried out at RCCS (Okazaki, Japan) and ACCMS (Kyoto University).

Keywords: Carbon dioxide fixation · Cyclic carbonates · DFT calculation · Epoxides · Porphyrinoids

[1] a) M. Cokoja, C. Bruckmeier, B. Rieger, W. A. Herrmann, F. E. Kühn, *Angew. Chem. Int. Ed.* **2011**, *50*, 8510–8537; *Angew. Chem.* **2011**, *123*, 8662–8690; b) Y. Tsuji, T. Fujihara, *Chem. Commun.* **2012**, *48*, 9956–9964; c) D. J. Darensbourg, S. J. Wilson, *Green Chem.* **2012**, *14*, 2665–2671; d) N. Kielland, C. J. Whiteoak, A. W. Kleij, *Adv. Synth. Catal.* **2013**, *355*, 2115–2138; e) C. Maeda, Y. Miyazaki, T. Ema, *Catal. Sci. Technol.* **2014**, *4*, 1482–1497; f) A. Tlili, E. Blondiaux, X. Frogneux, T. Cantat, *Green Chem.* **2015**, *17*, 157–168; g) Q. Liu, L. Wu, R. Jackstell, M. Beller, *Nature Commun.* **2015**, *6*, 5933–5947; h) J. W. Comerford, I. D. V. Ingram, M. North, X. Wu, *Green Chem.* **2015**, *17*, 1966–1987; i) C. Martín, G. Fiorani, A. W. Kleij, *ACS Catal.* **2015**, *5*, 1353–1370; j) M. Cokoja, M. E. Wilhelm, M. H. Anthofer, W. A. Herrmann, F. E. Kühn, *ChemSusChem* **2015**, *8*, 2436–2454.

[2] a) T. Aida, S. Inoue, *J. Am. Chem. Soc.* **1983**, *105*, 1304-1309; b) W. J. Kruper, D. D. Dellar, *J. Org. Chem.* **1995**, *60*, 725–727; c) R. L. Paddock, Y. Hiyama, J. M. McKay, S. T. Nguyen, *Tetrahedron Lett.* **2005**, *45*, 2023-2026; d) L. Jin, H. Jing, T. Chang, X. Bu, L. Wang, Z. Liu, *J. Mol. Catal. A: Chem.* **2007**, *261*, 262-266; e) F. Ahmadi, S. Tangestaninejad, M. Moghadam, V. Mirkhani, I. Mohammadpoor-Baltork, A. R. Khosropour, *Inorg. Chem. Commun.* **2011**, *14*, 1489-1493; f) B. Li, L. Zhang, Y. Song, D. Bai, H. Jing, *J. Mol. Catal. A: Chem.* **2012**, *363*, 26-30; g) Y. Qin, H. Guo, X. Sheng, X. Wang, F. Wang, *Green Chem.* **2015**, *17*, 2853-2858; h) A. Chen, Y. Zhang, J. Chen, L. Chen, Y. Yu, *J. Mater. Chem. A* **2015**, *3*, 9807-9816.

[3] a) T. Ema, Y. Miyazaki, S. Koyama, Y. Yano, T. Sakai, *Chem. Commun.* **2012**, *48*, 4489-4491; b) T. Ema, Y. Miyazaki, J. Shimonishi, C. Maeda, J. Hasegawa, *J. Am. Chem. Soc.* **2014**, *136*, 15270-15279; c) C. Maeda, T. Taniguchi, K. Ogawa, T. Ema, *Angew. Chem. Int. Ed.* **2015**, *54*, 134-138; *Angew. Chem.* **2015**, *127*, 136–140; d) C. Maeda, J. Shimonishi, R. Miyazaki, J. Hasegawa, T. Ema, *Chem. Eur. J.* **2016**, *in press. doi 10.1002/chem.201600164*.

[4] a) H. Sun, D. Zhang, *J. Phys. Chem. A* **2007**, *111*, 8036–8043; b) J. Q. Wang, K. Dong, W. G. Cheng, J. Sun, S. J. Zhang, *Catal. Sci. Technol.* **2012**, *2*, 1480-1484; c) J. Q. Wang, J. Sun, W. G. Cheng, K. Dong, X. P. Zhang, S. J. Zhang, *Phys. Chem. Chem. Phys.* **2012**, *14*, 11021-11026; d) S. Foltran, R. Mereau, T. Tassaing, *Catal. Sci. Technol.* **2014**, *4*, 1585-1597; e) C. C. Rocha, T. Onfroy, J. Pilme, A. Denicourt-Nowicki, A. Roucoux, F. Launay, *J. Catal.* **2016**, *333*, 29-39; f) Y. Li, L. Wang, T. F. Huang, J. L. Zhang, H. Q. He, *Ind. Eng. Chem. Res.* **2015**, *54*, 8093-8099; g) J. Ma, J. L. Liu, Z. F. Zhang, B. X. Han, *Green Chem.* **2012**, *14*, 2410-2420; h) C. J. Whiteoak, A. Nova, F. Maseras, A. W. Kleij, *ChemSusChem* **2012**, *5*, 2032-2038; i) Q. Wang, C. H. Guo, J. F. Jia, H. S. Wu, *J. Mol. Mod.* **2015**, *21*; j) F. Castro-Gomez, G. Salassa, A. W. Kleij, C. Bo, *Chem. Eur. J.* **2013**, *19*, 6289-6298; k) C. J. Whiteoak, N. Kielland, V. Laserna, F. Castro-Gomez, E. Martin, E. C. Escudero-Adan, C. Bo, A. W. Kleij, *Chem. Eur. J.* **2014**, *20*, 2264-2275; l) V. D'Elia, H. L. Dong, A. J. Rossini, C. M. Widdifield, S. V. C. Vummaleti, Y. Minenkov, A. Poater, E. Abou-Hamad, J. D. A. Pelletier, L. Cavallo, L. Emsley, J. M. Basset, *J. Am. Chem. Soc.* **2015**, *137*, 7728-7739.

[5] T. Ema, K. Fukuhara, T. Sakai, M. Ohbo, F.-Q. Bai, J. Hasegawa, *Cat. Sci. Technol.* **2015**, *5*, 2314-2321.

[6] a) C. Lee, W. Yang, R. G. Parr, *Phys Rev B* **1988**, *37*, 785-789; b) A. D. Becke, *J. Chem. Phys.* **1993**, *98*, 5648-5652.

[7] J. Tomasi, B. Mennucci, R. Cammi, *Chem. Rev.* **2005**, *105*, 2999-3093.

[8] W. Chen, W. L. Hase, H. B. Schlegel, *Chem. Phys. Lett.* **1994**, *228*, 436-442.

[9] J. J. P. Stewart, *J. Comp. Chem.* **1989**, *10*, 209-220.

[10] a) A. E. Reed, R. B. Weinstock, F. Weinhold, *J. Chem. Phys.* **1985**, *83*, 735-746; b) A. E. Reed, L. A. Curtiss, F. Weinhold, *Chem. Rev.* **1988**, *88*, 899-926.

[11] M. J. Frisch, G. W. Trucks, H. B. Schlegel, G. E. Scuseria, M. A. Robb, J. R. Cheeseman, G. Scalmani, V. Barone, B. Mennucci, G. A. Petersson, H. Nakatsuji, M. Caricato, X. Li, H. P. Hratchian, A. F. Izmaylov, J. Bloino, G. Zheng, J. L. Sonnenberg, M. Hada, M. Ehara, K. Toyota, R. Fukuda, J. Hasegawa, M. Ishida, T. Nakajima, Y. Honda, O. Kitao, H. Nakai, T. Vreven, J. Montgomery, J. A., J. E. Peralta, F. Ogliaro, M. Bearpark, J. J. Heyd, E. Brothers, K. N. Kudin, V. N. Staroverov, R. Kobayashi, J. Normand, K. Raghavachari, A. Rendell, J. C. Burant, S. S. Iyengar, J. Tomasi, M. Cossi, N. Rega, J. M. Millam, M. Klene, J. E. Knox, J. B. Cross, V. Bakken, C. Adamo, J. Jaramillo, R. Gomperts, R. E. Stratmann, O. Yazyev, A. J. Austin, R. Cammi, C. Pomelli, J. W. Ochterski, R. L. Martin, K. Morokuma, V. G. Zakrzewski, G. A. Voth, P. Salvador, J. J. Dannenberg, S. Dapprich, A. D. Daniels, Ö. Farkas, J. B. Foresman, J. V. Ortiz, J. Cioslowski, D. J. Fox, Gaussian, Inc., Wallingford CT, **2009**.

[12] *CRC Handbook of Chemistry and Physics, 75 th edition*, D. R. Lide ed., CRC Press, Florida, USA, **1994**.

Entry for the Table of Contents

PERSONAL ACCOUNT

Highly active bifunctional metalloporphyrin catalysts were developed for the reactions of epoxides with CO_2 to produce cyclic carbonates. The bifunctional catalysts have the metal center and the quaternary ammonium halide. DFT calculations were performed to elucidate the reaction mechanism. The results were consistent with the experimental data and useful for understanding the structure–activity relationship.

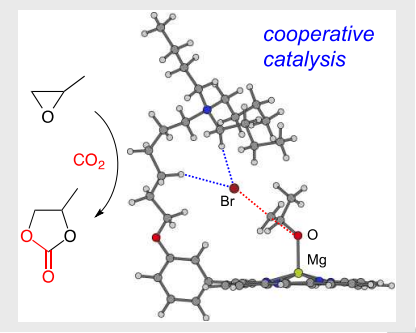

J. Hasegawa, R. Miyazaki, C. Maeda*, and T. Ema**

Page No. – Page No.

Theoretical Study on Highly Active Bifunctional Metalloporphyrin Catalysts for the Coupling Reaction of Epoxides with Carbon Dioxide